Centralized Cooperative Positioning from Euclidean Distance Matrices: Multidimensional Scaling and Maximum Likelihood

Eric Chaumette
ISAE-SUPAERO/University of Toulouse
Toulouse, France
eric.chaumette@isae-supaero.fr

Jordi Vilà-Valls
ISAE-SUPAERO/University of Toulouse
Toulouse, France
jordi.vila-valls@isae-supaero.fr

Yoan Gregoire
Centre National d'Études Spatiales
Toulouse, France
yoan.gregoire@cnes.fr

***Abstract*—In a plethora of applications that involve sensing networks or systems with multiple agents, it is fundamental to obtain reliable and complete positioning information. Considering a network of agents, this contribution focuses on the centralized cooperative positioning problem exploiting inter-agent ranging measurements, i.e., Euclidean distance matrix, and where only a subset of agents are able to estimate their position (and associated covariance) in a global frame. In that context, a standard solution is given by the multidimensional scaling and mapping (MDS-MAP) algorithm. In this article, an alternative maximum likelihood estimation approach is proposed, which improves the MDS-MAP performance and ensures asymptotical efficiency. An illustrative example is provided to support the discussion.**

***Index Terms*—Cooperative positioning, maximum likelihood estimation, multidimensional scaling, Cramée-Rao bound, Euclidean distance matrix.**

I. INTRODUCTION

Intelligent transportation systems [1], location-based services, the internet-of-things and wireless sensor networks [2]–[4], or distributed sensing systems for scientific missions (e.g., largely distributed sensor arrays [5] and future satellite swarms for radio interferometry in space [6]), to name a few, require reliable and precise positioning information for their successful operation. Such information, when the sensors of interest are on Earth, outdoors and affected by nominal conditions, is obtained through Global Navigation Satellite Systems [7], being nowadays the cornerstone source of positioning data. But in many applications GNSS are partially or not available, and alternative localization techniques must be accounted for, typically exploiting other radiofrequency signals [4], [8], [9].

In the context of multiple agents or sensing networks (e.g., swarm of satellites/vehicles or distributed sensing systems), two positioning approaches exist. In the typical cooperative localization/positioning framework [1]–[4], [10], each agent in the network exploits both local and external information, the latter received from neighboring (aiding) agents, in order to compute its own position. On the other hand, some applications require to estimate the position of all agents at once, in order to preserve the inherent geometry constraints, for network control tasks, or other application-dependent requirements (e.g., measurement synchronization in distributed instruments), that is, localization of the complete set in a centralized manner. This contribution focuses on the centralized localization problem, where the main assumptions are that, i) only a subset of agents are able to estimate their position (and associated covariance), and ii) inter-agent ranging is available for all agents in the network, that is, we consider a complete Euclidean distance matrix (EDM) [11].

A possible solution is given by the maximum likelihood estimator (MLE), which is known to be asymptotically efficient (i.e., in the large sample and/or high signal-to-noise ratio regimes [12], [13]), that is, its mean square error (MSE) tends to the Cramér-Rao bound (CRB). A problem with the MLE is its computational complexity, and that it requires a good initialization to obtain the global solution. An alternative is to resort to multidimensional scaling and mapping (MDS-MAP), a suboptimal two-step solution that is less computationally demanding and easily implementable (refer to [14] and references therein). In this article we show that the MDS-MAP estimate is asymptotically at the vicinity of the global minimum of the MLE cost function, leading to a feasible MLE Gauss-Newton implementation. An illustrative example is given to show that i) a symmetrized MDS outperforms the standard MDS; ii) while the MLE is efficient, the MDS-MAP is not; and iii) there exists a limit on the achievable precision that depends on the observations' variance.

II. SYSTEM MODEL AND PROBLEM FORMULATION

The system is composed of N sensing devices. Let $\mathbf{X} = [\mathbf{x}_1 \ \ldots \ \mathbf{x}_N] \in \mathbb{R}^{D \times N}$, $\{\mathbf{x}_n\}_{n=1}^N \in \mathbb{R}^D$, be the agents' position matrix to be estimated. In the ideal case, one may have access to the noise-free distances between all agents, $d_{n\to l} = \|\mathbf{x}_n - \mathbf{x}_l\|$, and the corresponding EDM is constructed from the squared distances as follows [11][1],

$$\mathbf{D} = \mathtt{edm}(\mathbf{X}) \Leftrightarrow [\mathbf{D}]_{n,l} = d_{n\to l}^2, \tag{1}$$

$$\mathbf{D} = \mathrm{diag}\left(\mathbf{X}^T\mathbf{X}\right)\mathbf{1}_N^T - 2\mathbf{X}^T\mathbf{X} + \mathbf{1}_N \mathrm{diag}\left(\mathbf{X}^T\mathbf{X}\right)^T. \tag{2}$$

This work was supported by the Centre National d'Études Spatiales (CNES), and the DGA/AID project 2022.65.0082.

[1] $\mathbf{I}_N$ is the identity matrix of dimension N, and $\mathbf{1}_N$ is a N-dimensional vector where all components are equal to 1.

Notice that $\mathbf{D}$ is invariant to a translation, $\mathtt{edm}(\mathbf{X}) = \mathtt{edm}\left(\mathbf{X}-\mathbf{x}_0\mathbf{1}_N^T\right), \forall \mathbf{x}_0 \in \mathbb{R}^D$; and to a unitary transformation, $\mathtt{edm}(\mathbf{X}) = \mathtt{edm}(\mathbf{UX}), \forall \mathbf{U} \in \mathbb{R}^{D\times D} \mid \mathbf{U}^T\mathbf{U} = \mathbf{U}\mathbf{U}^T = \mathbf{I}_D$. This implies that $\mathbf{X}$ cannot be identified in a global frame using only $\mathbf{D}$. A possible solution is to consider a known position for a subset of agents, $N' \leq N$, i.e., $\mathbf{X} = [\mathbf{X}_{N'}\ \mathbf{X}_{N-N'}] \in \mathbb{R}^{D\times N}$, with known $\mathbf{X}_{N'}$ and unknown $\mathbf{X}_{N-N'}$.

In practice, both N' agents' position and inter-agent distances are estimated, and distances may be asymmetric, $\widehat{d}_{n\to l} \neq \widehat{d}_{l\to n}$. Under a zero-mean Gaussian noise assumption,

$$\begin{aligned} \widehat{d}_{n\to l} &= \|\mathbf{x}_n - \mathbf{x}_l\| + n_{n,l} \sim \mathcal{N}\left(d_{n\to l}, \sigma_d^2\right), \\ \widehat{\mathbf{x}}_{n'} &= \mathbf{x}_{n'} + \mathbf{n}_{n'} \sim \mathcal{N}\left(\mathbf{x}_{n'}, \sigma_p^2 \mathbf{I}_D\right), \end{aligned} \tag{3}$$

which leads to an estimated subset $\widehat{\mathbf{X}}_{N'} = [\widehat{\mathbf{x}}_1\ \ldots\ \widehat{\mathbf{x}}_{N'}]$ and estimated EDM $\widehat{\mathbf{D}}$, with $[\widehat{\mathbf{D}}]_{n,l} = \widehat{d}^2_{n\to l}$.

The problem is the estimation of $\mathbf{X}$ from EDM $\widehat{\mathbf{D}}$, and considering the estimated subset of positions $\widehat{\mathbf{X}}_{N'}$.

III. Multidimensional Scaling and Mapping

The MDS-MAP is a two-step algorithm that provides a solution to the problem stated above:

- *Step 1 - MDS:* Position computation in a local reference frame using inter-agent distances, i.e., from the EDM.
- *Step 2 - MAP:* Position transformation into a real frame using position estimates of a subset of agents, i.e., estimate a translation vector and orthonormal matrix to transform the estimated local positions into absolute ones.

A. Ideal MDS-MAP

In the ideal case, we have access to $\mathbf{D}$ and $\mathbf{X}_{N'}$. If we consider a generic translation $\mathbf{x_s} = \mathbf{Xs},\ \mathbf{s} \in \mathbb{R}^{N\times 1}$,

$$\mathbf{Y^s} = \mathbf{X} - \mathbf{x_s}\mathbf{1}_N^T = \mathbf{X}\left(\mathbf{I}_N - \mathbf{s}\mathbf{1}_N^T\right), \tag{4}$$

and under the condition $\mathbf{1}_N^T\mathbf{s} = 1$,

$$\left(\mathbf{Y^s}\right)^T\mathbf{Y^s} = -\frac{1}{2}\left(\mathbf{I}_N - \mathbf{1}_N\mathbf{s}^T\right)\mathbf{D}\left(\mathbf{I}_N - \mathbf{s}\mathbf{1}_N^T\right) = \mathbf{D^s}. \tag{5}$$

$\mathbf{Y^s}$ admits a SVD, $\mathbf{Y^s} = \mathbf{U^s}\mathbf{\Sigma^s}\left(\mathbf{V^s}\right)^T$, and then

$$\left(\mathbf{Y^s}\right)^T\mathbf{Y^s} = \mathbf{V^s}\left(\mathbf{\Sigma^s}\right)^T\mathbf{\Sigma^s}\left(\mathbf{V^s}\right)^T = \mathbf{D^s}, \mathbf{\Sigma^s} \in \mathbb{R}^{D\times N}, \tag{6}$$

where $rank\left(\mathbf{\Sigma^s}\right) = rank\left(\mathbf{Y^s}\right) \leq \min\{D, N\}$. One can identify $\mathbf{\Sigma^s}$ and $\mathbf{V^s}$ by performing an EVD on $\mathbf{D^s}$, and

$$\begin{aligned} \mathbf{Z^s} = \mathbf{\Sigma^s}\left(\mathbf{V^s}\right)^T &\Leftrightarrow \mathbf{Y^s} = \mathbf{U^s}\mathbf{Z^s} \\ &\Leftrightarrow \mathbf{X} = \mathbf{U^s}\mathbf{Z^s} + \left(\mathbf{Xs}\right)\mathbf{1}_N^T, \end{aligned} \tag{7}$$

which implies that $\mathbf{Z^s}$ leads to matrix $\mathbf{X}$, now unknown with respect to a translation and unitary transformation.

In the MAP step we exploit the known positions $\mathbf{X}_{N'}$. If we consider $\mathbf{Z^s} = \left[\mathbf{Z^s}_{N'}\ \mathbf{Z^s}_{N-N'}\right]$ and $\mathbf{\Pi}^{\perp}_{\mathbf{1}_{N'}} = \mathbf{I}_{N'} - \frac{\mathbf{1}_{N'}\mathbf{1}_{N'}^T}{N'}$,

$$\mathbf{X}_{N'} = \mathbf{U^s}\mathbf{Z^s}_{N'} + \left(\mathbf{Xs}\right)\mathbf{1}_{N'}^T, \tag{8}$$

$$\mathbf{X}_{N'}\mathbf{\Pi}^{\perp}_{\mathbf{1}_{N'}} = \mathbf{U^s}(\mathbf{Z^s}_{N'}\mathbf{\Pi}^{\perp}_{\mathbf{1}_{N'}}),\ \text{(centered positions).} \tag{9}$$

$\mathbf{U^s}$ is obtained from the singular value decomposition (SVD) of $\mathbf{Z^s}_{N'}\mathbf{\Pi}^{\perp}_{\mathbf{1}_{N'}}\mathbf{X}_{N'}^T$,

$$\begin{aligned} (\mathbf{Z^s}_{N'}\mathbf{\Pi}^{\perp}_{\mathbf{1}_{N'}})(\mathbf{X}_{N'}\mathbf{\Pi}^{\perp}_{\mathbf{1}_{N'}})^T = \mathbf{Z^s}_{N'}\mathbf{\Pi}^{\perp}_{\mathbf{1}_{N'}}\mathbf{X}_{N'}^T = \mathbf{\Phi^s}\mathbf{\Upsilon^s}\left(\mathbf{\Psi^s}\right)^T \\ \Rightarrow \mathbf{\Psi^s}\left(\mathbf{\Phi^s}\right)^T = \mathbf{U^s},\ \text{iff } N' \geq D+1 \text{ and} \qquad (10) \\ rank(\mathbf{Z^s}_{N'}\mathbf{\Pi}^{\perp}_{\mathbf{1}_{N'}}) = rank(\mathbf{X}_{N'}\mathbf{\Pi}^{\perp}_{\mathbf{1}_{N'}}) = D, \qquad (11) \end{aligned}$$

and from (8) the translation is $\mathbf{Xs} = (\mathbf{X}_{N'} - \mathbf{U^s}\mathbf{Z^s}_{N'})\frac{\mathbf{1}_{N'}}{N'}$.

$\mathbf{X}$ can be identified from an ideal EDM $\mathbf{D}$ only if $N' \geq (D+1)$ positions are known and $rank(\mathbf{X}_{N'}\mathbf{\Pi}^{\perp}_{\mathbf{1}_{N'}}) = D$,

$$\mathbf{X} = \mathbf{U^s}\mathbf{Z^s} + \left((\mathbf{X}_{N'} - \mathbf{U^s}\mathbf{Z^s}_{N'})\frac{\mathbf{1}_{N'}}{N'}\right)\mathbf{1}_N^T. \tag{12}$$

B. MDS-MAP from noisy observations

In practice, we only have access to the estimated $\widehat{\mathbf{D}}$ and $\widehat{\mathbf{X}}_{N'}$. Under this condition, can one still use the MDS-MAP algorithm detailed in the previous Sec. III-A? We have now that $\widehat{\mathbf{D}}^{\mathbf{s}} = -\frac{1}{2}\left(\mathbf{I}_N - \mathbf{1}_N\mathbf{s}^T\right)\widehat{\mathbf{D}}\left(\mathbf{I}_N - \mathbf{s}\mathbf{1}_N^T\right)$, and the problem can be reformulated as follows,

$$(\widehat{\mathbf{V}}^{\mathbf{s}}, \widehat{\mathbf{\Sigma}}^{\mathbf{s}}) = \arg\min_{(\mathbf{V},\mathbf{\Sigma})}\left\{\left\|\mathbf{V}\left(\mathbf{\Sigma}^T\mathbf{\Sigma}\right)\mathbf{V}^T - \widehat{\mathbf{D}}^{\mathbf{s}}\right\|_F^2\right\}, \tag{13a}$$

$$\widehat{\mathbf{Z}}^{\mathbf{s}} = \widehat{\mathbf{\Sigma}}^{\mathbf{s}}(\widehat{\mathbf{V}}^{\mathbf{s}})^T, \widehat{\mathbf{Y}}^{\mathbf{s}} = \widehat{\mathbf{U}}^{\mathbf{s}}\widehat{\mathbf{\Sigma}}^{\mathbf{s}}(\widehat{\mathbf{V}}^{\mathbf{s}})^T, \tag{13b}$$

$$\widehat{\mathbf{U}}^{\mathbf{s}} = \arg\min_{\substack{\mathbf{U}\in\mathbb{R}^{D\times D}\\ \mathbf{U}^T\mathbf{U}=\mathbf{I}_D}}\left\{\left\|\widehat{\mathbf{X}}_{N'}\mathbf{\Pi}^{\perp}_{\mathbf{1}_{N'}} - \mathbf{U}\widehat{\mathbf{Z}}^{\mathbf{s}}_{N'}\mathbf{\Pi}^{\perp}_{\mathbf{1}_{N'}}\right\|_F^2\right\}, \tag{13c}$$

with $\|\mathbf{A}\|_F$ the Frobenius norm of $\mathbf{A}$, $\|\mathbf{A}\|_F^2 = tr\left(\mathbf{A}^T\mathbf{A}\right)$. We can show that asymptotically (i.e., $\sigma_d^2 \to 0$ and $\sigma_p^2 \to 0$)

$$\lim_{\text{asymp}}\mathbb{E}[\|\widehat{\mathbf{D}} - \mathbf{D}\|_F^2] = 0,\ \lim_{\text{asymp}}\mathbb{E}[\|\widehat{\mathbf{X}}_{N'} - \mathbf{X}_{N'}\|_F^2] = 0,$$

then $(\widehat{\mathbf{V}}^{\mathbf{s}}, \widehat{\mathbf{\Sigma}}^{\mathbf{s}}, \widehat{\mathbf{U}}^{\mathbf{s}})$ are consistent estimators of $(\mathbf{V^s}, \mathbf{\Sigma^s}, \mathbf{U^s})$. Therefore, $\lim_{\text{asymp}}\mathbb{E}[\|\widehat{\mathbf{X}}^{\mathbf{s}} - \mathbf{X}\|_F^2] = 0$, and

$$\widehat{\mathbf{X}}^{\mathbf{s}} = \widehat{\mathbf{U}}^{\mathbf{s}}\widehat{\mathbf{Z}}^{\mathbf{s}} + \left((\widehat{\mathbf{X}}_{N'} - \widehat{\mathbf{U}}^{\mathbf{s}}\widehat{\mathbf{Z}}^{\mathbf{s}}_{N'})\frac{\mathbf{1}_{N'}}{N'}\right)\mathbf{1}_N^T. \tag{13d}$$

In the general case with asymmetric estimated distances, $\widehat{d}_{n\to l} \neq \widehat{d}_{l\to n}$, (13a) must be modified because $\mathbf{V}\left(\mathbf{\Sigma}^T\mathbf{\Sigma}\right)\mathbf{V}^T$ is a symmetric matrix, then being a constraint on the solution. In that case, we consider a symmetrized matrix (and the eigenvalue decomposition (EVD)), i.e.,

$$\widehat{\mathbf{D}}^{\mathbf{s}} \to \frac{\widehat{\mathbf{D}}^{\mathbf{s}} + (\widehat{\mathbf{D}}^{\mathbf{s}})^T}{2}.$$

Notice that the identifiability conditions on $(\widehat{\mathbf{V}}^{\mathbf{s}}, \widehat{\mathbf{\Sigma}}^{\mathbf{s}}, \widehat{\mathbf{U}}^{\mathbf{s}})$ is $N' \geq D+1$ and $rank(\widehat{\mathbf{X}}_{N'}\mathbf{\Pi}^{\perp}_{\mathbf{1}_{N'}}) = D$, which leads to $rank(\widehat{\mathbf{Z}}^{\mathbf{s}}) = rank(\widehat{\mathbf{Y}}^{\mathbf{s}}) = D$. One may consider two possible implementations of the MDS-MAP, detailed in Algorithm 1.

It is important to notice that

$$\mathbb{E}[[\widehat{\mathbf{D}}]_{n,l}] = \mathbb{E}[\widehat{d}^2_{n\to l}] = d^2_{n\to l} + \sigma^2_{n\to l}, \tag{14}$$

$$\mathbb{E}[\widehat{\mathbf{D}}] = \mathbf{D} + \mathbf{\Sigma}_d, \tag{15}$$

Algorithm 1: MDS-MAP from noisy observations

Input: $\widehat{\mathbf{D}}$ and $\widehat{\mathbf{X}}_{N'}$.
Construct $\widehat{\mathbf{D}}^{\mathbf{s}} = -\frac{1}{2}\left(\mathbf{I}_N - \mathbf{1}_N\mathbf{s}^T\right)\widehat{\mathbf{D}}\left(\mathbf{I}_N - \mathbf{s}\mathbf{1}_N^T\right)$
Case 1: Standard MDS (SVD)
 $\widehat{\mathbf{D}}^{\mathbf{s}} = \widehat{\boldsymbol{\Omega}}\widehat{\boldsymbol{\Sigma}}\widehat{\mathbf{V}}^T$, $\widehat{\mathbf{Z}}^{\mathbf{s}} = \widehat{\boldsymbol{\Sigma}}^{\mathbf{s}}(\widehat{\mathbf{V}}^{\mathbf{s}})^T$ with $(\widehat{\boldsymbol{\Sigma}}^{\mathbf{s}}, \widehat{\mathbf{V}}^{\mathbf{s}})$ associated to the D largest singular values.
Case 2: Symmetrized MDS (EVD)
 $\frac{\widehat{\mathbf{D}}^{\mathbf{s}}+(\widehat{\mathbf{D}}^{\mathbf{s}})^T}{2} = \widehat{\mathbf{V}}\widehat{\boldsymbol{\Sigma}}^T\widehat{\boldsymbol{\Sigma}}\widehat{\mathbf{V}}^T$, $\widehat{\mathbf{Z}}^{\mathbf{s}} = \widehat{\boldsymbol{\Sigma}}^{\mathbf{s}}(\widehat{\mathbf{V}}^{\mathbf{s}})^T$ with $(\widehat{\boldsymbol{\Sigma}}^{\mathbf{s}}, \widehat{\mathbf{V}}^{\mathbf{s}})$ associated to the D largest eigenvalues.
MAP (SVD)
 $\widehat{\mathbf{Z}}^{\mathbf{s}}_{N'}\boldsymbol{\Pi}^{\perp}_{\mathbf{1}_{N'}}\widehat{\mathbf{X}}^T_{N'} = \widehat{\boldsymbol{\Phi}}\widehat{\boldsymbol{\Upsilon}}\widehat{\boldsymbol{\Psi}}$, $\widehat{\mathbf{U}}^{\mathbf{s}} = \widehat{\boldsymbol{\Psi}}^{\mathbf{s}}(\widehat{\boldsymbol{\Phi}}^{\mathbf{s}})^T$ with $(\widehat{\boldsymbol{\Psi}}^{\mathbf{s}}, \widehat{\boldsymbol{\Phi}}^{\mathbf{s}})$ associated to the D largest singular values.
MDS-MAP
 $\widehat{\mathbf{X}}^{\mathbf{s}} = \widehat{\mathbf{U}}^{\mathbf{s}}\widehat{\mathbf{Z}}^{\mathbf{s}} + \left(\left(\widehat{\mathbf{X}}_{N'} - \widehat{\mathbf{U}}^{\mathbf{s}}\widehat{\mathbf{Z}}^{\mathbf{s}}_{N'}\right)\frac{\mathbf{1}_{N'}}{N'}\right)\mathbf{1}_N^T$
Return: $\widehat{\mathbf{X}}^{\mathbf{s}}$

where $\boldsymbol{\Sigma}_d$ is a covariance matrix, including the case where $\sigma^2_{n\to l}$ may not be the same for different distance estimates. Then, $\widehat{\mathbf{D}}$ is a biased estimate of $\mathbf{D}$, which a priori leads to a biased estimate $\widehat{\mathbf{X}}^{\mathbf{s}}$. In order to compensate such bias, one should replace $\widehat{\mathbf{D}}$ by $\widehat{\mathbf{D}} - \boldsymbol{\Sigma}_d$. In practice, if $\sigma^2_{n\to l} \ll d^2_{n\to l}$, the bias induced by the estimated EDM is negligible.

IV. A Maximum Likelihood Approach to Centralized Cooperative Positioning

The observation model (3) is a Gaussian conditional signal model, for which the MLE is the asymptotically best estimator in the MSE sense. Despite nearly optimal properties, this estimator typically suffers from a large computational cost, as it may require solving a nonlinear multidimensional optimization problem. In the sequel, we derive the MLE for centralized positioning, and propose a feasible implementation.

A. Maximum likelihood estimator

If we gather the unknowns in vector $\boldsymbol{\theta} = \mathbf{vec}(\mathbf{X})$, define $\widehat{\mathbf{B}} = (\widehat{\mathbf{D}})^{1/2}$, and considering $D = 3$, the likelihood is,

$$p(\widehat{\mathbf{B}}, \widehat{\mathbf{X}}_{N'}; \boldsymbol{\theta}) = p(\widehat{\mathbf{B}}; \boldsymbol{\theta})p(\widehat{\mathbf{X}}_{N'}; \boldsymbol{\theta}), \tag{16}$$

$$p(\widehat{\mathbf{B}}; \boldsymbol{\theta}) = \left(2\pi\sigma_d^2\right)^{-\frac{(N-1)N}{2}} e^{-\frac{1}{2\sigma_d^2}\sum\limits_{n=1}^{N}\sum\limits_{l=1, l\neq n}^{N}\left(\widehat{d}_{n\to l} - \|\mathbf{x}_n - \mathbf{x}_l\|\right)^2},$$

$$p(\widehat{\mathbf{X}}_{N'}; \boldsymbol{\theta}) = \left(2\pi\sigma_p^2\right)^{-\frac{3N'}{2}} e^{-\frac{1}{2\sigma_p^2}\sum\limits_{n'=1}^{N'}\|\widehat{\mathbf{x}}_{n'} - \mathbf{x}_{n'}\|^2},$$

and the MLE $\widehat{\boldsymbol{\theta}}_{\text{ML}}$ of $\boldsymbol{\theta}$ is given by,

$$\begin{aligned}\widehat{\boldsymbol{\theta}}_{\text{ML}} &= \arg\max_{\boldsymbol{\theta}}\left\{p(\widehat{\mathbf{B}}, \widehat{\mathbf{X}}_{N'}; \boldsymbol{\theta})\right\} \\ &= \arg\min_{\boldsymbol{\theta}}\left\{\mathcal{C}(\widehat{\mathbf{B}}, \widehat{\mathbf{X}}_{N'}; \boldsymbol{\theta})\right\},\end{aligned} \tag{17}$$

$$\mathcal{C}(\widehat{\mathbf{B}}, \widehat{\mathbf{X}}_{N'}; \boldsymbol{\theta}) = \mathcal{C}^d(\widehat{\mathbf{B}}; \boldsymbol{\theta}) + \mathcal{C}^p(\widehat{\mathbf{X}}_{N'}; \boldsymbol{\theta}), \tag{18}$$

$$\mathcal{C}^d(\widehat{\mathbf{B}}; \boldsymbol{\theta}) = \frac{1}{2\sigma_d^2}\sum_{n=1}^{N}\sum_{l=1, l\neq n}^{N}\left(\widehat{d}_{n\to l} - \|\mathbf{x}_n - \mathbf{x}_l\|\right)^2,$$

$$\mathcal{C}^p(\widehat{\mathbf{X}}_{N'}; \boldsymbol{\theta}) = \frac{1}{2\sigma_p^2}\sum_{n'=1}^{N'}\|\widehat{\mathbf{x}}_{n'} - \mathbf{x}_{n'}\|^2.$$

The cost function $\mathcal{C}(\cdot) \triangleq \mathcal{C}(\widehat{\mathbf{B}}, \widehat{\mathbf{X}}_{N'}; \boldsymbol{\theta})$ does not allow to obtain a closed-form MLE, and looking for the solution on a grid in the parameters' space $\mathbb{R}^{3N}$ is not feasible.

B. On the MLE implementation

Taking into account the consistency of the MDS-MAP estimator $\widehat{\boldsymbol{\theta}}^{\mathbf{s}} = \mathbf{vec}(\widehat{\mathbf{X}}^{\mathbf{s}})$ (under the identifiability conditions given in Sec. III-B), and the consistency of the MLE,

$$\lim_{\text{asymp}}\mathbb{E}_{\boldsymbol{\theta}}[\|\widehat{\boldsymbol{\theta}}^{\mathbf{s}} - \boldsymbol{\theta}\|^2] = 0, \ \lim_{\text{asymp}}\mathbb{E}_{\boldsymbol{\theta}}[\|\widehat{\boldsymbol{\theta}}_{\text{ML}} - \boldsymbol{\theta}\|^2] = 0, \tag{19}$$

$$\|\widehat{\boldsymbol{\theta}}_{\text{ML}} - \widehat{\boldsymbol{\theta}}^{\mathbf{s}}\| \leq \|\widehat{\boldsymbol{\theta}}^{\mathbf{s}} - \boldsymbol{\theta}\| + \|\widehat{\boldsymbol{\theta}}_{\text{ML}} - \boldsymbol{\theta}\|, \tag{20}$$

therefore,

$$\lim_{\text{asymp}}\mathbb{E}_{\boldsymbol{\theta}}[\|\widehat{\boldsymbol{\theta}}_{\text{ML}} - \widehat{\boldsymbol{\theta}}^{\mathbf{s}}\|^2] = 0. \tag{21}$$

The MDS-MAP estimator $\widehat{\boldsymbol{\theta}}^{\mathbf{s}}$ is asymptotically at the vicinity of the global minimum of $\mathcal{C}(\cdot)$, that is, $\widehat{\boldsymbol{\theta}}^{\mathbf{s}}$ can be used to obtain $\widehat{\boldsymbol{\theta}}_{\text{ML}}$ through a Gauss-Newton approach. Indeed,

$$\begin{aligned}\frac{\partial\mathcal{C}(\widehat{\mathbf{B}}, \widehat{\mathbf{X}}_{N'}; \widehat{\boldsymbol{\theta}}_{\text{ML}})}{\partial\boldsymbol{\theta}} &\simeq \frac{\partial\mathcal{C}(\widehat{\mathbf{B}}, \widehat{\mathbf{X}}_{N'}; \widehat{\boldsymbol{\theta}}^{\mathbf{s}})}{\partial\boldsymbol{\theta}} \\ &+ \frac{\partial^2\mathcal{C}(\widehat{\mathbf{B}}, \widehat{\mathbf{X}}_{N'}; \widehat{\boldsymbol{\theta}}^{\mathbf{s}})}{\partial\boldsymbol{\theta}^T\partial\boldsymbol{\theta}}(\widehat{\boldsymbol{\theta}}_{\text{ML}} - \widehat{\boldsymbol{\theta}}^{\mathbf{s}}),\end{aligned} \tag{22}$$

and then,

$$\widehat{\boldsymbol{\theta}}_{\text{ML}} \simeq \widehat{\boldsymbol{\theta}}^{\mathbf{s}} - \left(\frac{\partial^2\mathcal{C}(\widehat{\mathbf{B}}, \widehat{\mathbf{X}}_{N'}; \widehat{\boldsymbol{\theta}}^{\mathbf{s}})}{\partial\boldsymbol{\theta}\partial\boldsymbol{\theta}^T}\right)^{-1}\frac{\partial\mathcal{C}(\widehat{\mathbf{B}}, \widehat{\mathbf{X}}_{N'}; \widehat{\boldsymbol{\theta}}^{\mathbf{s}})}{\partial\boldsymbol{\theta}}. \tag{23}$$

The Gauss-Newton MLE in (23) uses the instantaneous Hessian, but it has been shown [15], [16], that considering its mean value leads to a more stable solution,

$$\widehat{\boldsymbol{\theta}}_{\text{ML}} \simeq \widehat{\boldsymbol{\theta}}^{\mathbf{s}} - \left(\mathbb{E}_{\boldsymbol{\theta}}\left[\frac{\partial^2\mathcal{C}(\widehat{\mathbf{B}}, \widehat{\mathbf{X}}_{N'}; \widehat{\boldsymbol{\theta}}^{\mathbf{s}})}{\partial\boldsymbol{\theta}\partial\boldsymbol{\theta}^T}\right]\right)^{-1}\frac{\partial\mathcal{C}(\widehat{\mathbf{B}}, \widehat{\mathbf{X}}_{N'}; \widehat{\boldsymbol{\theta}}^{\mathbf{s}})}{\partial\boldsymbol{\theta}}. \tag{24}$$

C. Computing the gradient, the Hessian and its mean

The gradient of interest in (23) and (24) is given by,

$$\frac{\partial\mathcal{C}(\widehat{\mathbf{B}}, \widehat{\mathbf{X}}_{N'}; \boldsymbol{\theta})}{\partial\boldsymbol{\theta}} = \frac{\partial\mathcal{C}^d(\widehat{\mathbf{B}}; \boldsymbol{\theta})}{\partial\boldsymbol{\theta}} + \frac{\partial\mathcal{C}^p(\widehat{\mathbf{X}}_{N'}; \boldsymbol{\theta})}{\partial\boldsymbol{\theta}}, \tag{25}$$

$$\begin{cases}\frac{\partial\mathcal{C}^d(\cdot)}{\partial\mathbf{x}_n} = \frac{2}{\sigma_d^2}\sum\limits_{l=1, l\neq n}^{N}\left(\|\mathbf{x}_n - \mathbf{x}_l\| - \frac{\widehat{d}_{n\to l} + \widehat{d}_{l\to n}}{2}\right)\frac{\mathbf{x}_n - \mathbf{x}_l}{\|\mathbf{x}_n - \mathbf{x}_l\|} \\ \frac{\partial\mathcal{C}^p(\cdot)}{\partial\mathbf{x}_{n'}} = \frac{1}{\sigma_p^2}\left(\mathbf{x}_{n'} - \widehat{\mathbf{x}}_{n'}\right)\end{cases}$$

The corresponding Hessian and its mean value are,

$$\frac{\partial^2\mathcal{C}(\widehat{\mathbf{B}}, \widehat{\mathbf{X}}_{N'}; \boldsymbol{\theta})}{\partial\boldsymbol{\theta}\partial\boldsymbol{\theta}^T} = \frac{\partial^2\mathcal{C}^d(\widehat{\mathbf{B}}; \boldsymbol{\theta})}{\partial\boldsymbol{\theta}\partial\boldsymbol{\theta}^T} + \frac{\partial^2\mathcal{C}^p(\widehat{\mathbf{X}}_{N'}; \boldsymbol{\theta})}{\partial\boldsymbol{\theta}\partial\boldsymbol{\theta}^T}, \tag{26}$$

$$\begin{cases}\frac{\partial^2\mathcal{C}^d(\cdot)}{\partial\mathbf{x}_l\partial\mathbf{x}_n^T} = -\frac{2}{\sigma_d^2}\left(\boldsymbol{\Pi}_{\mathbf{x}_n - \mathbf{x}_l} + \left(1 - \frac{\widehat{d}_{n\to l} + \widehat{d}_{l\to n}}{2\|\mathbf{x}_n - \mathbf{x}_l\|}\right)\boldsymbol{\Pi}^{\perp}_{\mathbf{x}_n - \mathbf{x}_l}\right) \\ \frac{\partial^2\mathcal{C}^d(\cdot)}{\partial\mathbf{x}_n\partial\mathbf{x}_n^T} = \frac{2}{\sigma_d^2}\sum\limits_{l=1, l\neq n}^{N}\boldsymbol{\Pi}_{\mathbf{x}_n - \mathbf{x}_l} + \left(1 - \frac{\widehat{d}_{n\to l} + \widehat{d}_{l\to n}}{2\|\mathbf{x}_n - \mathbf{x}_l\|}\right)\boldsymbol{\Pi}^{\perp}_{\mathbf{x}_n - \mathbf{x}_l} \\ \frac{\partial^2\mathcal{C}^p(\cdot)}{\partial\mathbf{x}_{l'}\partial\mathbf{x}_{n'}^T} = \mathbf{0}_{3\times 3}, \\ \frac{\partial^2\mathcal{C}^p(\cdot)}{\partial\mathbf{x}_{n'}\partial\mathbf{x}_{n'}^T} = \frac{1}{\sigma_p^2}\mathbf{I}_3\end{cases}$$

$$\mathbb{E}_{\boldsymbol{\theta}}\left[\frac{\partial^2\mathcal{C}(\cdot)}{\partial\boldsymbol{\theta}\partial\boldsymbol{\theta}^T}\right] = \mathbb{E}_{\boldsymbol{\theta}}\left[\frac{\partial^2\mathcal{C}^d(\cdot)}{\partial\boldsymbol{\theta}\partial\boldsymbol{\theta}^T}\right] + \mathbb{E}_{\boldsymbol{\theta}}\left[\frac{\partial^2\mathcal{C}^p(\cdot)}{\partial\boldsymbol{\theta}\partial\boldsymbol{\theta}^T}\right], \quad (27)$$

$$\begin{cases} \mathbb{E}_{\boldsymbol{\theta}}\left[\frac{\partial^2\mathcal{C}^d(\cdot)}{\partial\mathbf{x}_l\partial\mathbf{x}_n^T}\right] = -\frac{2}{\sigma_d^2}\boldsymbol{\Pi}_{\mathbf{x}_n-\mathbf{x}_l} \\ \mathbb{E}_{\boldsymbol{\theta}}\left[\frac{\partial^2\mathcal{C}^d(\cdot)}{\partial\mathbf{x}_n\partial\mathbf{x}_n^T}\right] = \frac{2}{\sigma_d^2}\sum_{l=1,l\neq n}^{N}\boldsymbol{\Pi}_{\mathbf{x}_n-\mathbf{x}_l} \\ \mathbb{E}_{\boldsymbol{\theta}}\left[\frac{\partial^2\mathcal{C}^p(\cdot)}{\partial\mathbf{x}_{l'}\partial\mathbf{x}_{n'}^T}\right] = \mathbf{0}_{3\times3}, \\ \mathbb{E}_{\boldsymbol{\theta}}\left[\frac{\partial^2\mathcal{C}^p(\cdot)}{\partial\mathbf{x}_{n'}\partial\mathbf{x}_{n'}^T}\right] = \frac{1}{\sigma_p^2}\mathbf{I}_3 \end{cases}$$

where the orthogonal projector is $\boldsymbol{\Pi}_{\mathbf{x}_n-\mathbf{x}_l} = (\mathbf{x}_n-\mathbf{x}_l)(\mathbf{x}_n-\mathbf{x}_l)^T/\left\|\mathbf{x}_n-\mathbf{x}_l\right\|^2$, and $\boldsymbol{\Pi}^{\perp}_{\mathbf{x}_n-\mathbf{x}_l} = \mathbf{I}_3 - \boldsymbol{\Pi}_{\mathbf{x}_n-\mathbf{x}_l}$.

D. Cramér-Rao Bound

In order to evaluate the optimality of both MLE and MDS-MAP, it is interesting to compare the MSE with the corresponding CRB. For the Gaussian signal model of interest we can directly resort to the Slepian-Bangs formula [17] to compute the Fisher information matrix, $\mathbf{F}_{\boldsymbol{\theta}}$, which leads to $\mathbf{CRB}_{\boldsymbol{\theta}} = \mathbf{F}_{\boldsymbol{\theta}}^{-1}$. For the signal model (3), (16),

$$\mathbf{F}_{\boldsymbol{\theta}} = -\mathbb{E}_{\boldsymbol{\theta}}\left[\frac{\partial^2\ln p(\widehat{\mathbf{B}},\widehat{\mathbf{X}}_{N'};\boldsymbol{\theta})}{\partial\boldsymbol{\theta}\partial\boldsymbol{\theta}^T}\right] = \mathbf{F}_{\boldsymbol{\theta}}^d + \mathbf{F}_{\boldsymbol{\theta}}^p, \quad (28)$$

$$\mathbf{F}_{\boldsymbol{\theta}}^d = -\mathbb{E}_{\boldsymbol{\theta}}\left[\frac{\partial^2\ln p(\widehat{\mathbf{B}};\boldsymbol{\theta})}{\partial\boldsymbol{\theta}\partial\boldsymbol{\theta}^T}\right], \; \mathbf{F}_{\boldsymbol{\theta}}^p = -\mathbb{E}_{\boldsymbol{\theta}}\left[\frac{\partial^2\ln p(\widehat{\mathbf{X}}_{N'};\boldsymbol{\theta})}{\partial\boldsymbol{\theta}\partial\boldsymbol{\theta}^T}\right].$$

The first term $\mathbf{F}_{\boldsymbol{\theta}}^d$ has diagonal matrix terms $\mathbf{F}^d_{\mathbf{x}_n,\mathbf{x}_n}$, and off-diagonal ones $\mathbf{F}^d_{\mathbf{x}_n,\mathbf{x}_l}$:

$$\mathbf{F}^d_{\mathbf{x}_n,\mathbf{x}_l} = -\frac{2}{\sigma_d^2}\Pi_{\mathbf{x}_n-\mathbf{x}_l}, \; \mathbf{F}^d_{\mathbf{x}_n,\mathbf{x}_n} = \frac{2}{\sigma_d^2}\sum_{l=1,l\neq n}^{N}\Pi_{\mathbf{x}_n-\mathbf{x}_l}. \quad (29)$$

The second term is

$$\mathbf{F}_{\boldsymbol{\theta}}^p = \frac{1}{\sigma_p^2}\begin{bmatrix} \mathbf{I}_{3N'} & \mathbf{0} \\ \mathbf{0} & \mathbf{0} \end{bmatrix}. \quad (30)$$

It is interesting to notice that

$$\mathbb{E}_{\boldsymbol{\theta}}\left[\frac{\partial^2\mathcal{C}(\widehat{\mathbf{B}},\widehat{\mathbf{X}}_{N'};\boldsymbol{\theta})}{\partial\boldsymbol{\theta}\partial\boldsymbol{\theta}^T}\right] = \mathbf{F}_{\boldsymbol{\theta}}, \quad (31)$$

$$\lim_{\max\left\{\sigma_d^2,\sigma_p^2\right\}\to 0}\frac{\partial^2\mathcal{C}(\widehat{\mathbf{B}},\widehat{\mathbf{X}}_{N'};\boldsymbol{\theta})}{\partial\boldsymbol{\theta}\partial\boldsymbol{\theta}^T} = \mathbf{F}_{\boldsymbol{\theta}}. \quad (32)$$

V. VALIDATION

In order to assess the performance of the different methods we consider an illustrative cooperative positioning example, with a network of $N = 10$ agents, where $N' = 4$ (anchors) have access to an estimated position $\widehat{\mathbf{x}}_n$. All agents estimate the inter-agent distance, then leading to an asymmetric EDM $\widehat{\mathbf{D}}$. With $\mathbf{X}_{10} = [\mathbf{X}_4 \; \mathbf{X}_6]$, the position of the $N - N'$ agents $\mathbf{X}_6$ (tags) is randomly drawn in $\left[-\frac{\eta}{2}, \frac{\eta}{2}\right]$, and for the anchors,

$$\mathbf{X}_4 = \eta\begin{bmatrix} 0 & 1 & \cos(\phi) & \cos(\phi) \\ 0 & 0 & \sin(\phi) & 0 \\ 0 & 0 & 0 & \sin(\phi) \end{bmatrix}.$$

The CRB is compared to the MSE (from 10^4 Monte Carlo runs) obtained for the following four algorithms (we also compute the efficiency as eff = MSE/CRB):

- The standard MDS-MAP detailed in Algorithm 1, using the SVD (Case 1), named MDS-SVD-MAP.
- The symmetrized MDS-MAP detailed in Algorithm 1, using the EVD (Case 2), named MDS-EVD-MAP.
- The MLE in (24), initialized with the symmetrized MDS-MAP and with only 1 iteration for the Gauss-Newton.
- A clairvoyant MLE (CMLE), initialized with true system positions, and again with only 1 iteration.

First, we consider a particular example with $\sigma_p = 3$, $\sigma_d = 3$, $\phi = 45°$ and $\eta = 100$. The network configuration is shown in Fig. 1 (top plot). The MSE for the different methods, together with the CRB, is shown for this scenario in the middle plot of Fig. 1, and the corresponding efficiency in the bottom plot. The x axis, from 1 to 30, refer to the (x, y, z) components of each agent (i.e., 1 to 12 for $\mathbf{X}_4$, and 13 to 30 for $\mathbf{X}_6$). We can see that: i) the MSE of the symmetrized MDS-MAP is lower than the MSE of the standard MDS-MAP (in general always equal or lower); ii) both MLE and CMLE MSEs coincide with the CRB; and iii) using both methods improves the position estimates for $\mathbf{X}_4$ (i.e., $\sigma_p^2 = 9.54$dB). While the MLE is efficient, both MDS-MAP solutions are not.

In the sequel, we consider the MSE for the subsets $\mathbf{X}_4$ and $\mathbf{X}_6$ (instead of showing each coordinate as in Fig. 1), i.e., if we consider $\boldsymbol{\theta}_4 = \mathbf{vec}(\mathbf{X}_4)$, $\widehat{\boldsymbol{\theta}}_4 = \mathbf{vec}(\widehat{\mathbf{X}}_4)$, $\boldsymbol{\theta}_6 = \mathbf{vec}(\mathbf{X}_6)$ and $\widehat{\boldsymbol{\theta}}_6 = \mathbf{vec}(\widehat{\mathbf{X}}_6)$, then $\mathrm{MSE}_{\boldsymbol{\theta}_4} = \mathbb{E}[\|\widehat{\boldsymbol{\theta}}_4 - \boldsymbol{\theta}_4\|^2]$ and $\mathrm{MSE}_{\boldsymbol{\theta}_6} = \mathbb{E}[\|\widehat{\boldsymbol{\theta}}_6 - \boldsymbol{\theta}_6\|^2]$; the corresponding bounds are $\mathrm{CRB}_{\boldsymbol{\theta}_4} = tr\left(\mathbf{CRB}_{\boldsymbol{\theta}_4}\right)$ and $\mathrm{CRB}_{\boldsymbol{\theta}_6} = tr\left(\mathbf{CRB}_{\boldsymbol{\theta}_6}\right)$. The results are shown in Fig. 2, where the top plot gives the MSE results for both $\mathbf{X}_4$ and $\mathbf{X}_6$, for different values of σ_d, considering a fixed $\sigma_p = 1$; and the bottom plot gives the MSE results for different values of σ_p, considering a fixed $\sigma_d = 1$. First, we can see again in both cases that the MLE is efficient and the MDS-MAP is not. Also, it is interesting to notice that there exists a limit on the achievable precision that depends on the observations' variance: i) in the first case, with fixed $\sigma_p = 1$, when $\sigma_d^2 \to 0$ both $\mathrm{MSE}_{\boldsymbol{\theta}_4}$ and $\mathrm{MSE}_{\boldsymbol{\theta}_6}$ tend to a constant value (a limit linked to σ_p); ii) in the second case, with fixed $\sigma_d = 1$, when $\sigma_p^2 \to 0$ $\mathrm{MSE}_{\boldsymbol{\theta}_6}$ (the unknown positions) tends to a constant value (a limit linked to σ_d). In addition, while the $\mathrm{MSE}_{\boldsymbol{\theta}_4}$ tends to 0 for the MLE, it tends to a constant value for the MDS-MAP, departing from the CRB.

VI. CONCLUSIONS

The problem of interest was the localization of a network of agents, from estimated inter-agent distances, and considering position estimates for a subset of agents. Possible solutions to this problem are given by the MLE and MDS-MAP. It was shown that the MDS-MAP estimate is asymptotically at the vicinity of the global minimum of the MLE cost function, leading to a feasible MLE Gauss-Newton implementation. An illustrative example was used to show that while the MLE is efficient, the MDS-MAP is not. In addition, there exists a limit on the achievable precision that depends on the observations'

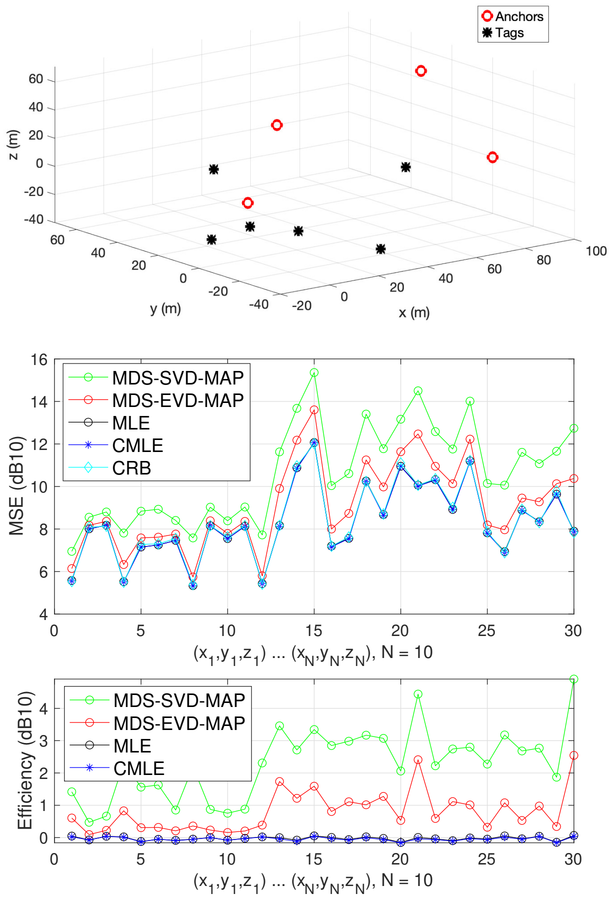

Figure 1: (Top) Position of the 10 agents; (Middle) MSE and (Bottom) efficiency for the standard MDS-MAP, symmetrized MDS-MAP, MLE and clairvoyant MLE.

variance, i.e., for a fixed σ_p^2 and $\sigma_d^2 \to 0$ the MSE does not tend to 0, and the same for a fixed σ_d^2 and $\sigma_p^2 \to 0$.

REFERENCES

[1] N. Alam and A. G. Dempster, "Cooperative Positioning for Vehicular Networks: Facts and Future," *IEEE Transactions on Intelligent Transportation Systems*, vol. 14, no. 4, pp. 1708–1717, Dec. 2013.

[2] N. Patwari et al., "Locating the Nodes: Cooperative Localization in Wireless Sensor Networks," *IEEE Signal Processing Magazine*, vol. 22, no. 4, pp. 54–69, 2005.

[3] H. Wymeersch, J. Lien, and M. Z. Win, "Cooperative Localization in Wireless Networks," *Proceedings of the IEEE*, vol. 97, no. 2, pp. 427–450, 2009.

[4] R. M. Buehrer, H. Wymeersch, and R. M. Vaghefi, "Collaborative Sensor Network Localization: Algorithms and Practical Issues," *Proceedings of the IEEE*, vol. 106, no. 6, pp. 1089–1114, June 2018.

[5] C. Ferrari et al., "French SKA White Book - The French community towards the Square Kilometre Array," *Published by the SKA-France Coordination in collaboration with AS SKA-LOFAR*, 2017.

[6] B. Cecconi et al., "NOIRE Study Report: Towards a Low Frequency Radio Interferometer in Space," in *Proc. IEEE Aerospace Conf.*, 2018.

[7] P. J. G. Teunissen and O. Montenbruck, Eds., *Handbook of Global Navigation Satellite Systems*, Springer, Switzerland, 2017.

[8] H. Wymeersch and G. Seco-Granados, "Radio Localization and Sensing – Part I: Fundamentals," *IEEE Communications Letters*, 2022.

[9] H. Wymeersch and G. Seco-Granados, "Radio Localization and Sensing – Part II: State-of-the-art and Challenges," *IEEE Communications Letters*, 2022.

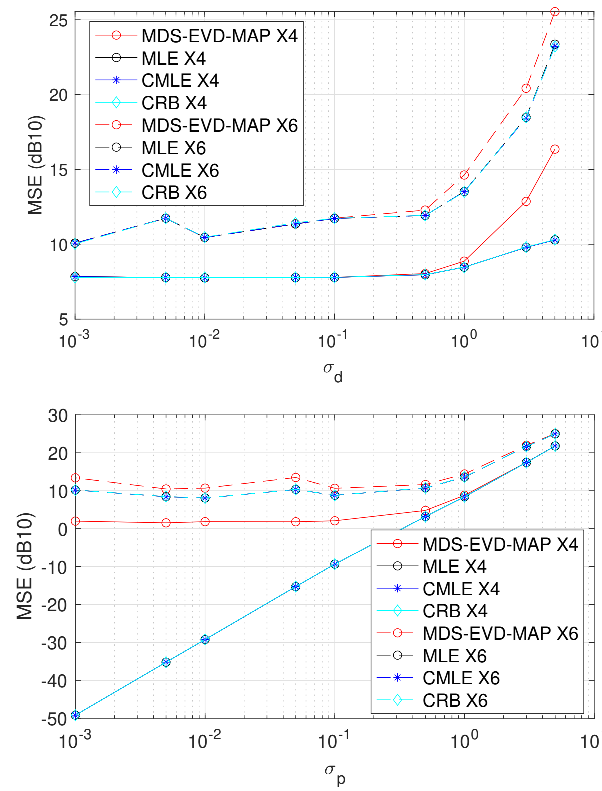

Figure 2: $\text{MSE}_{\boldsymbol{\theta}_4}$ (solid line) and $\text{MSE}_{\boldsymbol{\theta}_6}$ (dashed line) for the symmetrized MDS-MAP, MLE and CMLE, together with the CRB. Fixed $\sigma_p = 1$ (top) and fixed $\sigma_d = 1$ (bottom).

[10] D. Medina, L. Grundhöfer, and N. Hehenkamp, "Evaluation of Estimators for Hybrid GNSS-Terrestrial Localization in Collaborative Networks," in *Proc. IEEE Intl. Conf. on Intelligent Transportation Systems*, 2020.

[11] I. Dokmanic, R. Parhizkar, J. Ranieri, and M. Vetterli, "Euclidean Distance Matrices: Essential Theory, Algorithms, and Applications," *IEEE Signal Processing Magazine*, vol. 32, no. 6, pp. 12–30, 2015.

[12] P. Stoica and A. Nehorai, "Performances study of conditional and unconditional direction of arrival estimation," *IEEE Trans. Acoust., Speech, Signal Process.*, vol. 38, no. 10, pp. 1783–1795, Oct. 1990.

[13] A. Renaux, P. Forster, E. Chaumette, and P. Larzabal, "On the high-SNR conditional maximum-likelihood estimator full statistical characterization," *IEEE Trans. Signal Process.*, vol. 54, no. 12, pp. 4840 – 4843, Dec. 2006.

[14] N. Saeed, H. Nam, T. Y. Al-Naffouri, and M.-S. Alouini, "A State-of-the-Art Survey on Multidimensional Scaling-Based Localization Techniques," *IEEE Communications Surveys Tutorials*, vol. 21, no. 4, pp. 3565–3583, 2019.

[15] P. Stoica and A. Nehorai, "MUSIC, Maximum Likelihood, and Cramér-Rao Bound: Further Results and Comparisons," *IEEE Transactions on Acoustics, Speech, and Signal Processing*, vol. 38, no. 12, pp. 2140–2150, 1990.

[16] M. Viberg and B. Ottersten, "Sensor Array Processing Based on Subspace Fitting," *IEEE Trans. Signal Process.*, vol. 39, no. 5, pp. 1110–1121, 1991.

[17] S. M. Kay, *Fundamentals of Statistical Signal Processing: Estimation Theory*, Prentice-Hall, Englewood Cliffs, New Jersey, USA, 1993.